A Solid−State Dehydration Process in an Organic Material Associated with Substantial Hydrogen-Bond Reorganization, Investigated by Powder X-ray Diffraction

ARTICLE *in* CRYSTAL GROWTH & DESIGN · MAY 2010

Impact Factor: 4.89 · DOI: 10.1021/cg100330c

7 AUTHORS, INCLUDING:

Javier Marti-Rujas
Istituto Italiano di Tecnologia
40 PUBLICATIONS **429** CITATIONS
SEE PROFILE

Anabel Morte-Ródenas
Cardiff University
4 PUBLICATIONS **29** CITATIONS
SEE PROFILE

Benson Kariuki
Cardiff University
345 PUBLICATIONS **4,940** CITATIONS
SEE PROFILE

DOI: 10.1021/cg100330c

CRYSTAL GROWTH & DESIGN Article

2010, Vol. 10
3176–3181

A Solid-State Dehydration Process in an Organic Material Associated with Substantial Hydrogen-Bond Reorganization, Investigated by Powder X-ray Diffraction

Javier Martí-Rujas, Anabel Morte-Ródenas, Fang Guo, Nigel Thomas, Kotaro Fujii, Benson M. Kariuki, and Kenneth D. M. Harris*

School of Chemistry, Cardiff University, Park Place, Cardiff CF10 3AT, Wales

Received March 12, 2010; Revised Manuscript Received May 10, 2010

ABSTRACT: Solid *tert*-butylammonium acetate monohydrate undergoes a facile solid-state dehydration process under ambient conditions, in which single crystals of the monohydrate phase transform to a microcrystalline powder of an anhydrous product phase. The structural properties of the anhydrous phase have been determined directly from powder X-ray diffraction data, employing the direct-space genetic algorithm technique for structure solution followed by Rietveld refinement, allowing rationalization of the structural changes associated with the dehydration process. The dehydration process is associated with substantial reorganization of the hydrogen bonding arrangement, although one component of the hydrogen-bonding scheme is actually preserved in the transformation.

1. Introduction

Several different types of structural transformation[1] may occur in crystalline organic materials, including solid-state chemical reactions, transformations between polymorphic forms, processes involving solvent exchange, solvation, or desolvation among solvate and nonsolvate forms, and the formation of new materials by solid-state grinding (mechanochemical synthesis). Clearly, an essential prerequisite for understanding such transformations is to establish the details of the structural changes that take place. In favorable cases, transformations in crystalline materials proceed in a single crystal-to-single crystal manner,[2] such that a single crystal of the parent phase transforms into a single crystal of the product phase. In such cases, single-crystal X-ray diffraction may be exploited to monitor the structural changes associated with the transformation and, in particular, to determine the structure of the product phase. However, solid-state transformations often proceed instead with intrinsic loss of single-crystal integrity. In such cases, a single crystal of the parent phase typically yields a microcrystalline powder following the transformation, and structure determination of the product phase by single-crystal X-ray diffraction is not viable. Clearly, an alternative approach is required for structure determination, for example using powder X-ray diffraction, although it is important to recall that the task of carrying out structure determination of organic molecular solids directly from powder X-ray diffraction data[3] is significantly more challenging than structure determination from single-crystal X-ray diffraction. However, recent years have seen advances in the opportunities for carrying out structure determination of organic materials directly from powder X-ray diffraction data,[4] particularly due to the development of the direct-space strategy for structure solution.[4a] The emergence of these techniques provides a viable route for structural characterization of polycrystalline product phases produced directly by solid-state transformations of the type discussed above.[5] In the present work, we exploit these techniques (using an implementation of the direct-space genetic algorithm (GA) technique for structure solution[6]) to elucidate structural details of a solid-state dehydration process—in particular, dehydration of solid *tert*-butylammonium acetate monohydrate—that yields an anhydrous product phase as a microcrystalline powder. As discussed in more detail below, structural interest in materials such as *tert*-butylammonium acetate (and solvate phases thereof) is motivated in part by the aim of understanding the resultant crystal packing arrangements in materials for which there is *both* the opportunity to utilize strong hydrogen-bond donor and strong hydrogen-bond acceptor functionalities in the formation of favorable hydrogen-bonding arrangements *and* the need to address steric issues arising from the presence of bulky substituents (in this case the *tert*-butyl groups).

2. Materials Preparation and Analysis

Slow evaporation of solvent from a solution prepared by mixing *tert*-butylamine and dilute aqueous acetic acid (see Experimental Details) produced a crystalline material which was shown (from single-crystal X-ray diffraction and TGA analysis discussed below) to be a monohydrate phase of *tert*-butylammonium acetate. As no other hydrate phase of *tert*-butylammonium acetate is known, we subsequently refer to this material simply as the "hydrate phase". To date, we have been unable to obtain a pure (nonsolvate) crystalline phase of *tert*-butylammonium acetate by crystallization from solution. However, when the hydrate phase was exposed to the atmosphere at ambient temperature, it was observed (by optical microscopy) to lose single crystal integrity over a period of time of the order of an hour or so, resulting in a microcrystalline powder. Isothermal TGA studies (see Experimental Details) starting from the hydrate phase confirm that this transformation corresponds to complete loss of water (measured percentage mass loss, 11.88%; percentage mass of water in the hydrate phase, 11.92%). Powder X-ray diffraction (Figure 1) confirmed that the product was a new crystalline

*Author for correspondence. E-mail: HarrisKDM@cardiff.ac.uk.

Published on Web 05/27/2010

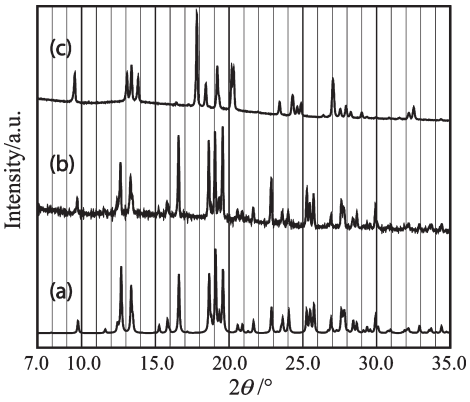

Figure 1. Comparison of powder X-ray diffraction patterns of (a) the hydrate phase (simulated from the crystal structure determined from single-crystal X-ray diffraction; see below), (b) the hydrate phase (experimental), and (c) the anhydrous phase (experimental; obtained by dehydration of the hydrate phase). Note that, due to the susceptibility of the hydrate phase to dehydration, the powder X-ray diffraction pattern for the hydrate phase in part b was recorded over a relatively short time and, hence, the signal/noise ratio is comparatively poor.

phase, with no detectable amounts of the parent hydrate phase present.

3. Structure Determination

The crystal structure of the hydrate phase has not been reported previously and was determined here by single-crystal X-ray diffraction (see Experimental Details and Supporting Information). The crystal structure (Figure 2) is monoclinic with space group $P2_1/n$ [$a = 7.6306(15)$ Å, $b = 18.094(4)$ Å, $c = 14.236(3)$ Å, $\beta = 98.57(3)°$; $V = 1943.65$ Å^3; calculated density, 1.033 g cm^{-3}]. The powder X-ray diffraction pattern simulated from this crystal structure is shown in Figure 1a. The good agreement between the simulated powder X-ray diffraction pattern for this structure (Figure 1a) and the experimental powder X-ray diffraction pattern for the bulk polycrystalline sample of the hydrate phase (Figure 1b) confirms that the structure of the hydrate phase determined from single-crystal X-ray diffraction data is fully representative of the bulk polycrystalline sample.

Structure determination of the anhydrous phase was carried out directly from powder X-ray diffraction data (see Experimental Details and Supporting Information). The powder X-ray diffraction pattern was indexed using the program TREOR,[7] giving the following unit cell with triclinic metric symmetry: $a = 6.43$ Å, $b = 7.19$ Å, $c = 10.05$ Å, $\alpha = 66.70°$, $\beta = 84.64°$, $\gamma = 83.15°$. Unit cell and profile refinement were carried out using the Le Bail fitting procedure,[8] giving good agreement between experimental and calculated powder X-ray diffraction profiles ($R_{wp} = 1.80\%$, $R_p = 1.31\%$) for this unit cell (Figure 3a). Density considerations suggest that the unit cell contains two *tert*-butylammonium cations and two acetate anions. Structure solution was carried out using the implementation of the direct-space GA technique in the program *EAGER*.[9] The GA structure solution calculations were carried out in space group $P\bar{1}$. With two *tert*-butylammonium cations and two acetate anions in the unit cell (see above), the asymmetric unit for $P\bar{1}$ comprises one *tert*-butylammonium cation and one acetate anion. In the GA calculation, the *tert*-butylammonium cation and acetate anion were each represented as rigid molecular fragments with hydrogen atoms

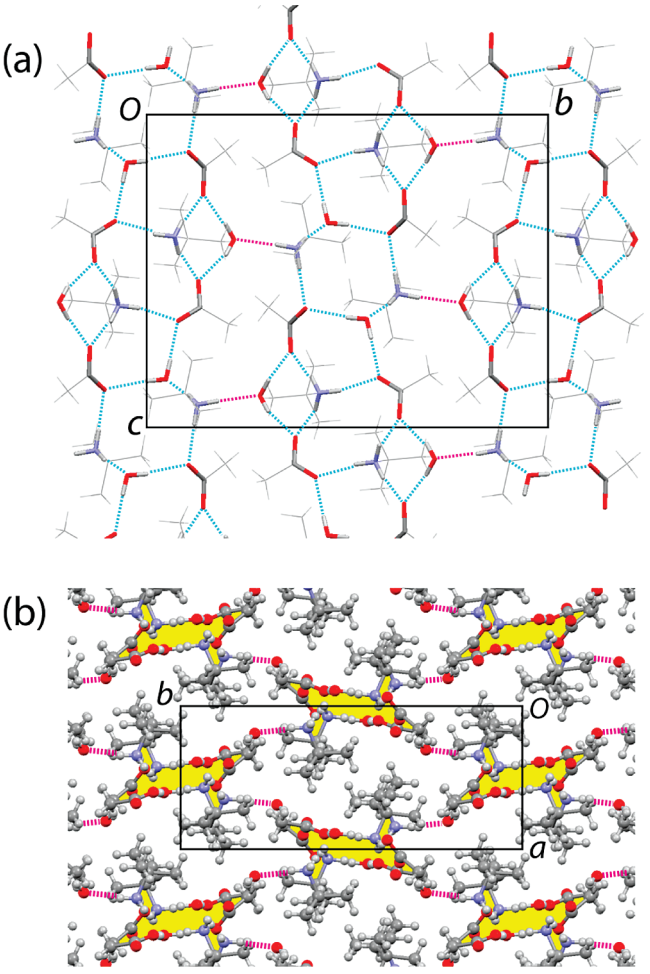

Figure 2. Crystal structure of the hydrate phase viewed (a) along the *a*-axis and (b) along the *c*-axis. Hydrogen bonds are indicated by dotted lines (blue dotted lines connect molecules within a given hydrogen-bonded ribbon, whereas red dotted lines connect adjacent ribbons). In part a, the groups engaged in hydrogen bonding are drawn with thicker bonds in order to highlight the hydrogen-bonding scheme. In part b, the ribbons are indicated by yellow shading, and red dotted lines represent hydrogen bonds between adjacent ribbons.

omitted. Thus, the total number of structural variables involved in the direct-space search was 12, comprising three translational variables $\{x, y, z\}$ and three orientational variables $\{\theta, \varphi, \psi\}$ for each fragment. The GA calculation was carried out for 50 generations, with a population size of 100 structures and with 25 mating operations and 10 mutation operations carried out in each generation. The best structure solution (i.e., the structure of lowest R_{wp} generated in the GA calculation) was used as the starting structural model for Rietveld refinement,[10] which was carried out using the GSAS program.[11] In the Rietveld refinement, standard geometric restraints were applied to bond lengths and bond angles (with the lengths of the two C−O bonds of the acetate anion restrained to be equal), and the restraints were relaxed gradually as the refinement progressed. The atomic positions were refined, together with a common isotropic displacement parameter for each molecular fragment. In the later stages of the refinement, hydrogen atoms were added to the structural model in positions corresponding to standard molecular geometries. For the NH_3^+ group of the *tert*-butylammonium cation, the positions of the hydrogen atoms corresponded to

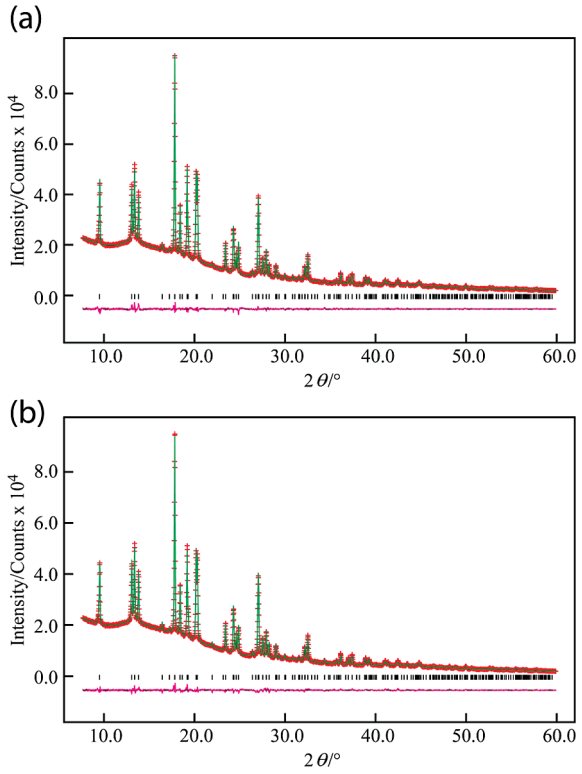

Figure 3. Results from (a) Le Bail fitting and (b) Rietveld refinement for the anhydrous phase. In each case, the plot shows the experimental (+), calculated (−), and difference (bottom) powder X-ray diffraction profiles. Reflection positions are marked.

geometrically reasonable N−H···O hydrogen bonds, as discussed in more detail below. The isotropic displacement parameter for each hydrogen atom was taken as 1.5 times that of the atom to which it is bonded. The final Rietveld refinement (Figure 3b) gave good agreement between calculated and experimental powder X-ray diffraction patterns (R_{wp} = 2.07%, R_p = 1.47%), with the following refined parameters: a = 6.42596(15) Å, b = 7.19411(17) Å, c = 10.04415(26) Å, α = 66.6999(13)°, β = 84.6295(15)°, γ = 83.1542(10)°; V = 422.873(23) Å^3; calculated density, 1.046 g cm^{-3} (2θ range, 7.69−59.93°; 3129 profile points; 119 refined variables). The crystal structure is shown in Figure 4.

4. Results and Discussion

The crystal structure of the hydrate phase (Figure 2) has two formula units of *tert*-butylammonium acetate and two water molecules in the asymmetric unit. The structure comprises a network of O−H···O and N−H···O hydrogen bonds, involving the water molecules and *tert*-butylammonium cations (O−H and N−H bonds, respectively) as hydrogen-bond donors and the acetate anions and water molecules (O atoms in each case) as hydrogen-bond acceptors. Each *tert*-butylammonium cation serves as the donor in three N−H···O hydrogen bonds, in one case involving three O atoms of acetate anions as the acceptors and in the other case involving two O atoms of water molecules and one O atom of an acetate anion as the acceptors. Each water molecule acts as the donor in two O−H···O hydrogen bonds (with O atoms of acetate anions as the acceptors in each case) and as the acceptor in one N−H···O hydrogen bond (with an N−H bond of a *tert*-butylammonium cation as the donor). The structure may be described as a three-dimensionally connected

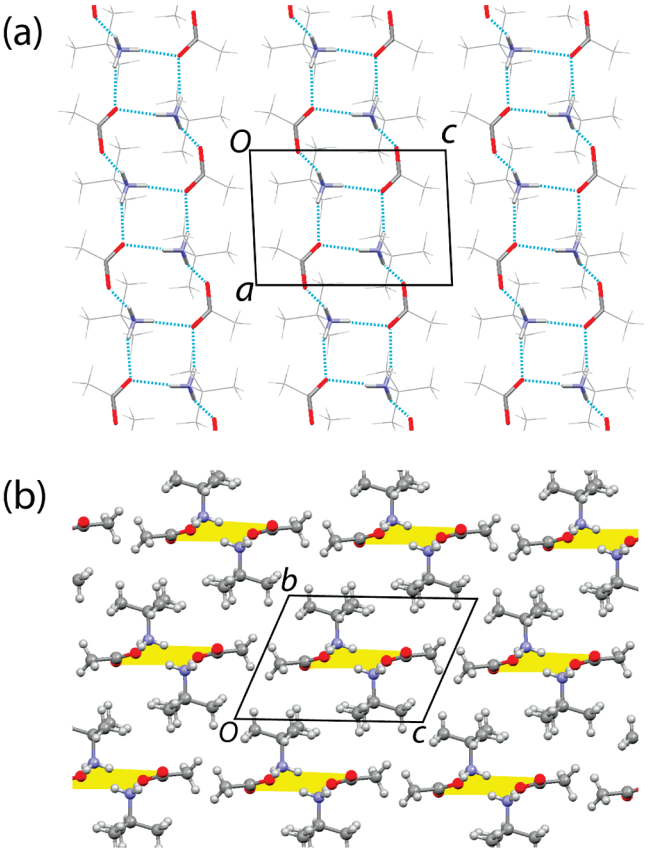

Figure 4. Crystal structure of the anhydrous phase viewed (a) along the *b*-axis and (b) along the *a*-axis. In part a, the groups engaged in hydrogen bonding are drawn with thicker bonds, and hydrogen bonds are indicated by blue dotted lines. In part b, the ribbons are indicated by yellow shading.

hydrogen bonded array. To facilitate the rationalization of this structure, however, it is convenient to identify ribbon-like hydrogen-bonded arrays that run parallel to the *c*-axis (vertical in Figure 2a). As shown in Figure 5a, these ribbons are constructed from four different types of cyclic hydrogen-bonded arrays (each involving four hydrogen bonds), described in graph set notation[12] as follows: (i) $R_4^4(12)$ [a centrosymmetric array, labeled (i) in Figure 5a, involving two *tert*-butylammonium cations and two acetate anions], (ii) $R_4^3(10)$ [labeled (ii) in Figure 5a, involving one *tert*-butylammonium cation and one water molecule as donors (utilizing two N−H bonds and two O−H bonds, respectively) and three O atoms of acetate anions as acceptors], (iii) $R_4^2(8)$ [labeled (iii) in Figure 5a, involving one *tert*-butylammonium cation and one water molecule as donors (utilizing two N−H bonds and two O−H bonds, respectively) and two O atoms of acetate anions as acceptors], and (iv) $R_6^4(12)$ [a centrosymmetric array, labeled (iv) in Figure 5a, involving two *tert*-butylammonium cations and two water molecules as donors (each utilizing two N−H bonds and one O−H bond, respectively) and two O atoms of acetate anions and two O atoms of water molecules as acceptors]. We note that the $R_4^4(12)$ array (which is the only cyclic array that does not involve water molecules) is retained[13] in the structure of the anhydrous phase discussed below. Each of these hydrogen-bonded ribbons is engaged in further hydrogen bonding (indicated by red dashed lines in Figure 5a) to adjacent ribbons lying in planes above and below, giving rise to a three-dimensionally connected hydrogen bonding network. When viewed along the *c*-axis (i.e., the direction of

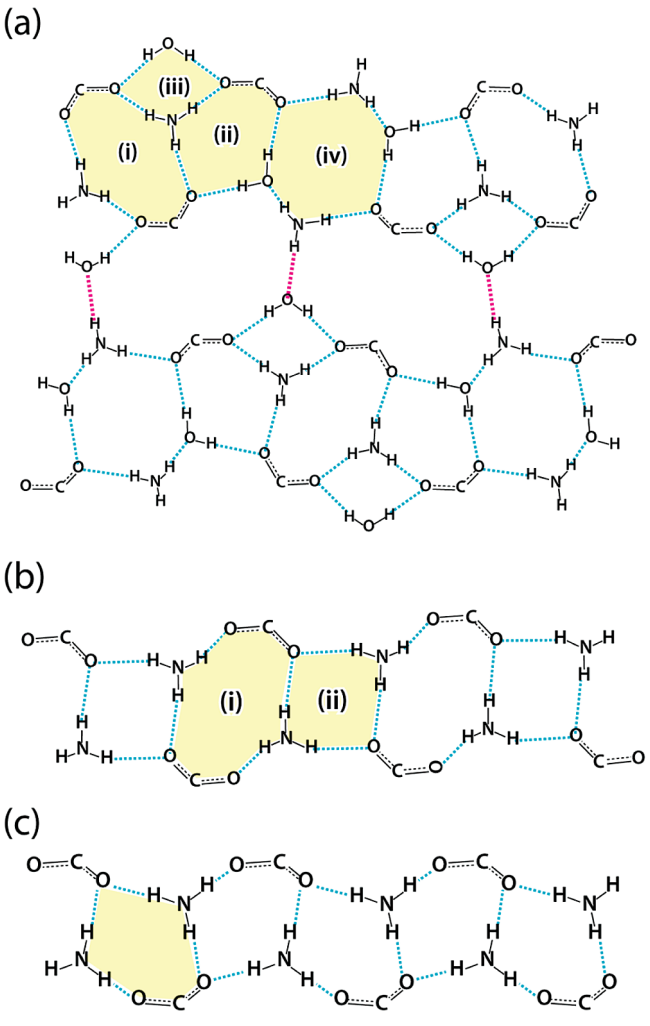

Figure 5. Schematic illustrations of (a) the hydrogen-bonding scheme in the hydrate phase, (b) the hydrogen-bonding scheme in the anhydrous phase, and (c) a hydrogen-bonding scheme commonly observed in other *tert*-butylammonium carboxylate materials. The hydrogen-bonded cycles shaded in yellow are discussed in the text.

propagation of the ribbons; Figure 2b), it is evident that this three-dimensional hydrogen-bonded network has a channel-like topology (the channels are parallel to the *c*-axis), with the *tert*-butyl groups of the *tert*-butylammonium cations accommodated within the channel-like region.

The crystal structure of the anhydrous phase (Figure 4) has one *tert*-butylammonium cation and one acetate anion in the asymmetric unit. Hydrogen-bonded ribbons (Figure 5b) propagate along the *a*-axis and are constructed from three independent types of N−H···O hydrogen bonds. All three N−H bonds of the *tert*-butylammonium cation serve as donors, one O atom of the acetate anion serves as a double acceptor, and the other O atom of the acetate anion serves as a single acceptor. Within the ribbon, there are two different types of cyclic hydrogen-bonded array, designated as $R_4^4(12)$ and $R_4^2(8)$ in graph set notation [labeled (i) and (ii), respectively, in Figure 5b]. There is a crystallographic inversion center at the center of each of these hydrogen-bonded cycles. The ribbons are not planar [although the non-hydrogen atoms involved in the hydrogen-bonded $R_4^2(8)$ cycle lie in the same plane, the non-hydrogen atoms involved in the hydrogen-bonded $R_4^4(12)$ cycle do not lie in the same plane and are arranged in a manner that resembles a "chair" configuration]. The mean plane of the hydrogen-bonding arrangement within each ribbon is parallel to the *ac*-plane. The methyl groups of the acetate anions and the *tert*-butyl groups of the *tert*-butylammonium cations project from the periphery of the ribbons (the methyl groups of the acetate anions are located approximately in the same plane as the hydrogen-bonding arrangement, whereas the *tert*-butyl groups project above and below this plane). As shown in Figure 4b (in which the structure is viewed parallel to the direction of propagation of the ribbons), each ribbon is surrounded by six others. However, in contrast to the situation observed for the hydrate phase, there is no hydrogen bonding between adjacent ribbons in the structure of the anhydrous phase. Instead, adjacent ribbons in the anhydrous phase interact only *via* van der Waals interactions involving the methyl and *tert*-butyl groups.

As noted above, the $R_4^4(12)$ hydrogen-bonded array in the structure of the anhydrous phase is also present in the structure of the hydrate phase, and it is conceivable that the integrity of this array is retained during the dehydration process. Nevertheless, the dehydration process is associated with significant changes to the overall hydrogen-bonding arrangement. In particular, as the water molecules are an integral part of the hydrogen-bonding arrangement in the hydrate phase, serving as both donors and acceptors, the loss of the water molecules in the dehydration process must inevitably disrupt the hydrogen-bonding, even though the hydrogen-bonding connectivity involving one of the two independent *tert*-butylammonium cations and one of the two independent acetate anions might remain intact during the transformation.

It is relevant to compare the structures reported here with those of other *tert*-butylammonium carboxylate materials (including hydrate and solvate phases). Of the structures within this class reported in the Cambridge Structural Database (CSD Version 5.31, November 2009), one structure (*tert*-butylammonium sorbate[14]) has an identical hydrogen-bonding arrangement to that reported here for the anhydrous phase of *tert*-butylammonium acetate, comprising hydrogen-bonded ribbons with an alternation of $R_4^4(12)$ and $R_4^2(8)$ hydrogen-bonded cycles. No other structure within this class has a hydrogen-bonding scheme that approaches the complexity of that observed here for the hydrate phase of *tert*-butylammonium acetate. However, the structure of one reported hydrate [tetrakis(*tert*-butylammonium)benzene-1,2,4,5-tetracarboxylate octahydrate[15]] does contain a hydrogen-bonded $R_4^3(10)$ cycle analogous to that observed within the hydrogen-bonding scheme of *tert*-butylammonium acetate hydrate (see above).

Among the structures of anhydrous *tert*-butylammonium carboxylate materials, however, the most common type of hydrogen-bonded ribbon[16] is one constructed entirely from $R_4^3(10)$ hydrogen-bonded cycles, involving two *tert*-butylammonium cations as donors (each utilizing two N−H bonds within the hydrogen-bonded cycle) and three O atoms of acetate anions as acceptors (with one O atom acting as the acceptor to two N−H···O hydrogen bonds). This hydrogen-bonded cycle is analogous to the $R_4^3(10)$ array observed in the hydrate phase of *tert*-butylammonium acetate, but with the two O−H donors of the water molecule replaced by two N−H donors from a *tert*-butylammonium cation (Figure 5c). In addition to the structures based on hydrogen-bonded ribbons, as discussed above, structures of *tert*-butylammonium carboxylate materials comprising cage-like hydrogen-bonding

arrangements, which serve as the host in solid inclusion compounds, have also been reported.[17]

Clearly, a more detailed rationalization of the preferred modes of molecular aggregation of *tert*-butylammonium carboxylate materials will rely on the application of appropriate computational techniques. Such computational studies would constitute an interesting subject for future research, particularly with a view to establishing a more quantitative understanding of the relative importance of optimizing the hydrogen-bonding arrangement *vis-à-vis* optimizing the steric effects due to the presence of the bulky *tert*-butyl groups in this family of materials.

5. Experimental Details

The hydrate phase of *tert*-butylammonium acetate was prepared by slow evaporation of solvent from a solution prepared by adding *tert*-butylamine (2.744 g) dropwise to dilute aqueous acetic acid (2.255 g of acetic acid in 11.38 g of water). Colorless crystals were formed with typical dimensions *ca.* $0.5 \times 0.5 \times 1$ mm^3. The material used for structure determination of the anhydrous phase of *tert*-butylammonium acetate was prepared by leaving several single crystals of the hydrate phase overnight in an oven at 25 °C [when the hydrate phase was left for a period of time at higher temperature (40 °C), sublimation was observed to occur].

Thermogravimetric analysis (TGA) was carried out on a TA Instruments Q600 Simultaneous TGA/DSC instrument. The isothermal TGA study of dehydration of the hydrate phase was carried out at 24 °C and led to complete loss of water after *ca.* 30 min at this temperature.

Crystal structure determination of the hydrate phase was carried out from single-crystal X-ray diffraction data collected on a Nonius Kappa CCD diffractometer at ambient temperature using monochromated Mo Kα radiation ($\lambda = 0.71073$ Å). Although an exposed sample of the hydrate phase undergoes dehydration over a period of an hour or so at ambient temperature, it was possible to collect single-crystal X-ray diffraction data sufficiently quickly for a crystal protected by a coating of inert oil such that the data were not significantly degraded. The crystal structure was solved and refined ($R1 = 0.0712$, $wR2 = 0.1570$ [$I > 2\sigma(I)$]) using SHELX97.[18] Refinement of non-hydrogen atoms was carried out with anisotropic displacement parameters. The positions of all hydrogen atoms in the hydrogen-bonding arrangement were revealed by difference Fourier analysis. The CH_3 and NH_3 groups were subsequently refined with an idealized geometry, and the isotropic displacement parameter for each hydrogen atom was taken as 1.5 times the equivalent isotropic displacement parameter of the atom to which it is bonded. Water molecules were refined with O−H distances loosely restrained, and the isotropic displacement parameter of each hydrogen atom was taken as 1.2 times the equivalent isotropic displacement parameter of the O atom to which it is bonded.

All powder X-ray diffraction experiments were carried out on a Bruker D8 diffractometer operating in transmission mode with Ge-monochromated Cu $K\alpha_1$ radiation ($\lambda = 1.5406$ Å) and a linear position-sensitive detector covering 12° in 2θ. In these transmission measurements, the sample was fixed between two pieces of adhesive tape in a foil-type sample holder (clearly, the X-ray scattering from the tape contributes to the measured powder X-ray diffraction pattern, giving rise to a significant background contribution that resembles the typical scattering from an amorphous component). For structure determination of the anhydrous phase, high-quality powder X-ray diffraction data were recorded on this instrument at ambient temperature, with a 2θ range 3.5−60°, a step size 0.017°, and a data collection time 12 h.

Acknowledgment. We are grateful to EPSRC and Cardiff University for financial support.

Supporting Information Available: CIF files containing crystallographic information for the hydrate phase and anhydrous phase of *tert*-butylammonium acetate. This material is available free of charge via the Internet at http://pubs.acs.org.

References

(1) (a) Thomas, J. M. *Philos. Trans. R. Soc. London* **1974**, *277*, 251. (b) Dunitz, J. D. *Acta Crystallogr., Sect. B* **1995**, *51*, 619. (c) Bernstein, J. *Polymorphism in Molecular Crystals*; Oxford University Press: Oxford, 2002. (d) Braga, D.; Grepioni, F. *Chem. Commun.* **2005**, 3635. (e) Herbstein, F. H. *Acta Crystallogr., Sect. B* **2006**, *62*, 341.

(2) (a) Nakanishi, H.; Jones, W.; Thomas, J. M. *Chem. Phys. Lett.* **1980**, *71*, 44. (b) Nakanishi, H.; Jones, W.; Thomas, J. M.; Hursthouse, M. B.; Motevalli, M. *J. Phys. Chem.* **1981**, *85*, 3636. (c) Enkelmann, V.; Wegner, G.; Novak, K.; Wagener, K. B. *J. Am. Chem. Soc.* **1993**, *115*, 10390. (d) Ohba, S.; Ito, Y. *Acta Crystallogr., Sect. E* **2003**, *59*, 149. (e) Chu, Q. L.; Swenson, D. C.; MacGillivray, L. R. *Angew. Chem., Int. Ed.* **2005**, *44*, 3569. (f) Friscic, T.; MacGillivray, L. R. *Z. Kristallogr.* **2005**, *220*, 351. (g) Koshima, H.; Kawanishi, H.; Nagano, M.; Yu, H. T.; Shiro, M.; Hosoya, T.; Uekusa, H.; Ohashi, Y. *J. Org. Chem.* **2005**, *70*, 4490. (h) Benedict, J. B.; Coppens, P. *J. Phys. Chem. A* **2009**, *113*, 3116. (i) Mir, M. H.; Koh, L. L.; Tan, G. K.; Vittal, J. J. *Angew. Chem., Int. Ed.* **2010**, *49*, 390.

(3) (a) David, W. I. F., Shankland, K., McCusker, L. B., Baerlocher, C., Eds. *Structure Determination from Powder Diffraction Data*; OUP/IUCr: **2002**. (b) Harris, K. D. M. *Cryst. Growth Des.* **2003**, *3*, 887. (c) Harris, K. D. M.; Cheung, E. Y. *Chem. Soc. Rev.* **2004**, *33*, 526. (d) Tremayne, M. *Philos. Trans. R. Soc. London* **2004**, *362*, 2691. (e) Černý, R. *Croat. Chem. Acta* **2006**, *79*, 319.

(4) (a) Harris, K. D. M.; Tremayne, M.; Lightfoot, P.; Bruce, P. G. *J. Am. Chem. Soc.* **1994**, *116*, 3543. (b) Chernyshev, V. V. *Russ. Chem. Bull.* **2001**, *50*, 2273. (c) Lightfoot, P.; Tremayne, M.; Harris, K. D. M.; Bruce, P. G. *J. Chem. Soc., Chem. Commun.* **1992**, 1012. (d) Kariuki, B. M.; Zin, D. M. S.; Tremayne, M.; Harris, K. D. M. *Chem. Mater.* **1996**, *8*, 565. (e) David, W. I. F.; Shankland, K.; Shankland, N. *Chem. Commun.* **1998**, 931. (f) Huq, A.; Stephens, P. W. *J. Pharm. Sci.* **2003**, *92*, 244. (g) Brunelli, M.; Wright, J. P.; Vaughan, G. R. M.; Mora, A. J.; Fitch, A. N. *Angew. Chem., Int. Ed.* **2003**, *42*, 2029. (h) Favre-Nicolin, V.; Černý, R. *Z. Kristallogr.* **2004**, *219*, 847. (i) Brodski, V.; Peschar, R.; Schenk, H. *J. Appl. Crystallogr.* **2005**, *38*, 688. (j) Tsue, H.; Horiguchi, M.; Tamura, R.; Fujii, K.; Uekusa, H. *J. Synth. Org. Chem. Jpn.* **2007**, *65*, 1203. (k) David, W. I. F.; Shankland, K. *Acta Crystallogr., Sect. A* **2008**, *64*, 52. (l) Altomare, A.; Caliandro, R.; Cuocci, C.; Giacovazzo, C.; Moliterni, A. G. G.; Rizzi, R.; Platteau, C. *J. Appl. Crystallogr.* **2008**, *41*, 56.

(5) (a) Cheung, E. Y.; Kitchin, S. J.; Harris, K. D. M.; Imai, Y.; Tajima, N.; Kuroda, R. *J. Am. Chem. Soc.* **2003**, *125*, 14658. (b) Mora, A. J.; Avila, E. E.; Delgado, G. E.; Fitch, A. N.; Brunelli, M. *Acta Crystallogr., Sect. B* **2005**, *61*, 96. (c) Platteau, C.; Lefebvre, J.; Affouard, F.; Willart, J. F.; Derollez, P.; Mallet, F. *Acta Crystallogr., Sect. B* **2005**, *61*, 185. (d) Guo, F.; Harris, K. D. M. *J. Am. Chem. Soc.* **2005**, *127*, 7314. (e) Hirano, S.; Toyota, S.; Toda, F.; Fujii, K.; Uekusa, H. *Angew. Chem., Int. Ed.* **2005**, *45*, 6013. (f) Guguta, C.; Meekes, H.; Gelder, R. *Cryst. Growth Des.* **2006**, *6*, 2686. (g) Albesa-Jové, D.; Pan, Z.; Harris, K. D. M.; Uekusa, H. *Cryst. Growth Des.* **2008**, *8*, 3641. (h) Guo, F.; Martí-Rujas, J.; Pan, Z.; Hughes, C. E.; Harris, K. D. M. *J. Phys. Chem. C* **2008**, *112*, 19793. (i) Hasegawa, G.; Komasaka, T.; Bando, R.; Yoshihashi, Y.; Yonemochi, E.; Fujii, K.; Uekusa, H.; Terada, K. *Int. J. Pharm.* **2009**, *369*, 12. (j) Fujii, K.; Ashida, Y.; Uekusa, H.; Hirano, S.; Toyota, S.; Toda, F.; Pan, Z.; Harris, K. D. M. *Cryst. Growth Des.* **2009**, *9*, 1201. (k) Fujii, K.; Uekusa, H.; Itoda, N.; Hasegawa, G.; Yonemochi, E.; Terada, K.; Pan, Z.; Harris, K. D. M. *J. Phys. Chem. C* **2010**, *114*, 580.

(6) (a) Kariuki, B. M.; Serrano-González, H.; Johnston, R. L.; Harris, K. D. M. *Chem. Phys. Lett.* **1997**, *280*, 189. (b) Harris, K. D. M.; Johnston, R. L.; Kariuki, B. M. *Acta Crystallogr., Sect. A* **1998**, *54*, 632. (c) Turner, G. W.; Tedesco, E.; Harris, K. D. M.; Johnston, R. L.; Kariuki, B. M. *Chem. Phys. Lett.* **2000**, *321*, 183. (d) Habershon, S.; Harris, K. D. M.; Johnston, R. L. *J. Comput. Chem.* **2003**, *24*, 1766. (e) Harris, K. D. M.; Habershon, S.; Cheung, E. Y.; Johnston, R. L. *Z. Kristallogr.* **2004**, *219*, 838.

(7) Werner, P.-E.; Eriksson, L.; Westdahl, M. *J. Appl. Crystallogr.* **1985**, *18*, 367.

(8) Le Bail, A.; Duroy, H.; Fourquet, J. L. *Mater. Res. Bull.* **1988** *23*, 447.

(9) (a) Tedesco, E.; Turner, G. W.; Harris, K. D. M.; Johnston, R. L.; Kariuki, B. M. *Angew. Chem., Int. Ed.* **2000**, *39*, 4488. (b) Tedesco, E.; Della Sala, F.; Favaretto, L.; Barbarella, G.; Albesa-Jové, D.; Pisignano, D.; Gigli, G.; Cingolani, R.; Harris, K. D. M. *J. Am. Chem. Soc.* **2003**, *125*, 12277. (c) Cheung, E. Y.; Harris, K. D. M.; Kang, T.; Scheffer, J. R.; Trotter, J. *J. Am. Chem. Soc.* **2006**, *128*, 15554. (d) Albesa-Jové, D.; Kariuki, B. M.; Kitchin, S. J.; Grice, L.; Cheung,

E. Y.; Harris, K. D. M. *ChemPhysChem* **2004**, *5*, 414. (e) Pan, Z.; Xu, M.; Cheung, E. Y.; Harris, K. D. M.; Constable, E. C.; Housecroft, C. E. *J. Phys. Chem. B* **2006**, *110*, 11620.

(10) (a) Rietveld, H. M. *J. Appl. Crystallogr.* **1969**, *2*, 65. (b) Young, R. A., Ed. *The Rietveld Method*; International Union of Crystallography: Oxford, 1993. (c) McCusker, L. B.; Von Dreele, R. B.; Cox, D. E.; Louër, D.; Scardi, P. *J. Appl. Crystallogr.* **1999**, *32*, 36.

(11) Larson A. C.; Von Dreele R. B. GSAS, Los Alamos Laboratory Report No. LA-UR-86-748, **1987**.

(12) (a) Etter, M. C. *Acc. Chem. Res.* **1990**, *23*, 120. (b) Etter, M. C.; MacDonald, J. C.; Bernstein, J. *Acta Crystallogr., Sect. B* **1990**, *46*, 256. (c) Bernstein, J.; Davis, R. E.; Shimoni, L.; Chang, N. L. *Angew. Chem., Int. Ed.* **1995**, *34*, 1555.

(13) We note that, in many other cases of dehydration processes in molecular crystals, the hydrogen bonding arrangement in the anhydrous product phase does not retain any common features with the hydrogen bonding arrangement in the parent hydrate phase.

(14) Nagahama, S.; Inoue, K.; Sada, K.; Miyata, M.; Matsumoto, A. *Cryst. Growth Des.* **2003**, *3*, 247.

(15) Ejsmont, K.; Zaleski, J. *Acta Crystallogr., Sect. E* **2007**, *63*, o4315.

(16) (a) Kinbara, K.; Kai, A.; Maekawa, Y.; Hashimoto, Y.; Naruse, S.; Hasegawa, M.; Saigo, K. *J. Chem. Soc., Perkin Trans.* **1996**, *2*, 247. (b) Cheung, E. Y.; David, S. E.; Harris, K. D. M.; Conway, B. R.; Timmins, P. *J. Solid State Chem.* **2007**, *180*, 1068. (c) Li, J.; Liang, Z. P.; Lin, C. H.; Tai, X. S. *Acta Crystallogr., Sect. E* **2008**, *64*, o2318.

(17) (a) Yuge, T.; Hisaki, I.; Miyata, M.; Tohnai, N. *CrystEngComm* **2008**, *10*, 263. (b) Sada, K.; Watanabe, T.; Miyamoto, J.; Fukuda, T.; Tohnai, N.; Miyata, M.; Kitayama, T.; Maehara, K.; Ute, K. *Chem. Lett.* **2004**, *33*, 160.

(18) Sheldrick, G. M. *SHELX97—Program for Crystal Structure Analysis* (*Release 97-2*); Institüt für Anorganische Chemie der Universität Göttingen: Tammanstrasse 4, D-3400 Göttingen, Germany, 1998.